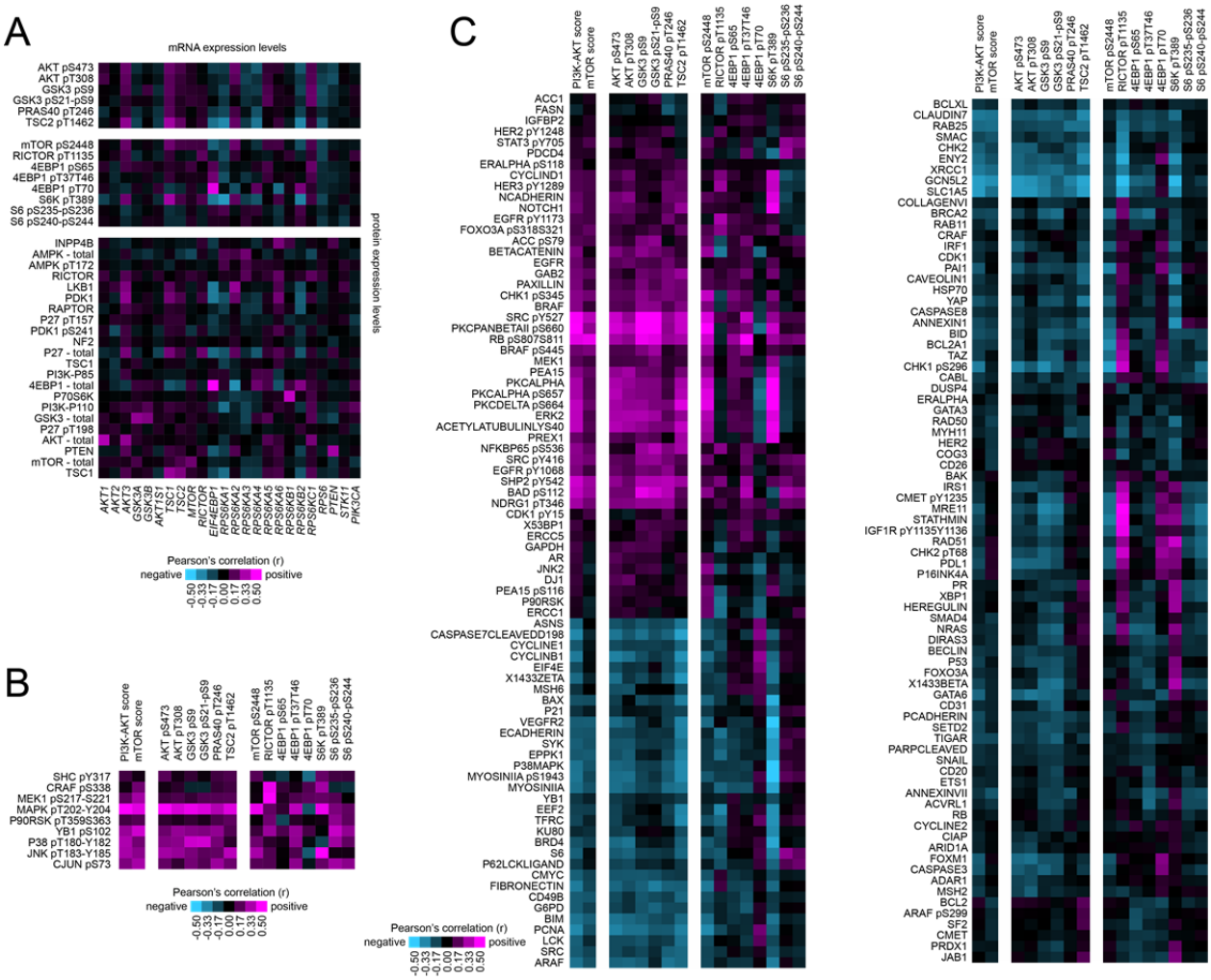

Figure S1, related to Figure 1. Correlations involving PI3K/AKT/mTOR RPPA features and mRNA features or other RPPA features. (A) Across all cancers, Pearson's correlations between PI3K/AKT/mTOR RPPA features (from Figure 1C) and mRNA expression of the associated genes. Correlations involve 7663 cancer cases with RPPA data available. **(B)** Across all cancers, Pearson's correlations between PI3K/AKT/mTOR RPPA features and MAP Kinase-related RPPA features. **(C)** Across all cancers, Pearson's correlations between PI3K/AKT/mTOR RPPA features and the other RPPA features represented in the dataset that are not related to PI3K/AKT/mTOR or MAP Kinase (i.e. RPPA features not represented in Figures 1C or S1B) but highly statistically significant (p<1E-6) for correlation with either PI3K/AKT or mTOR proteomic score.

Table S1, related to Figure 1. Summary of cancer cases examined in this study, according to data platform. Provided as an Excel file.

Table S2, related to Figure 1. By patient, data for key protein and RNA features examined in this study. Provided as an Excel file.

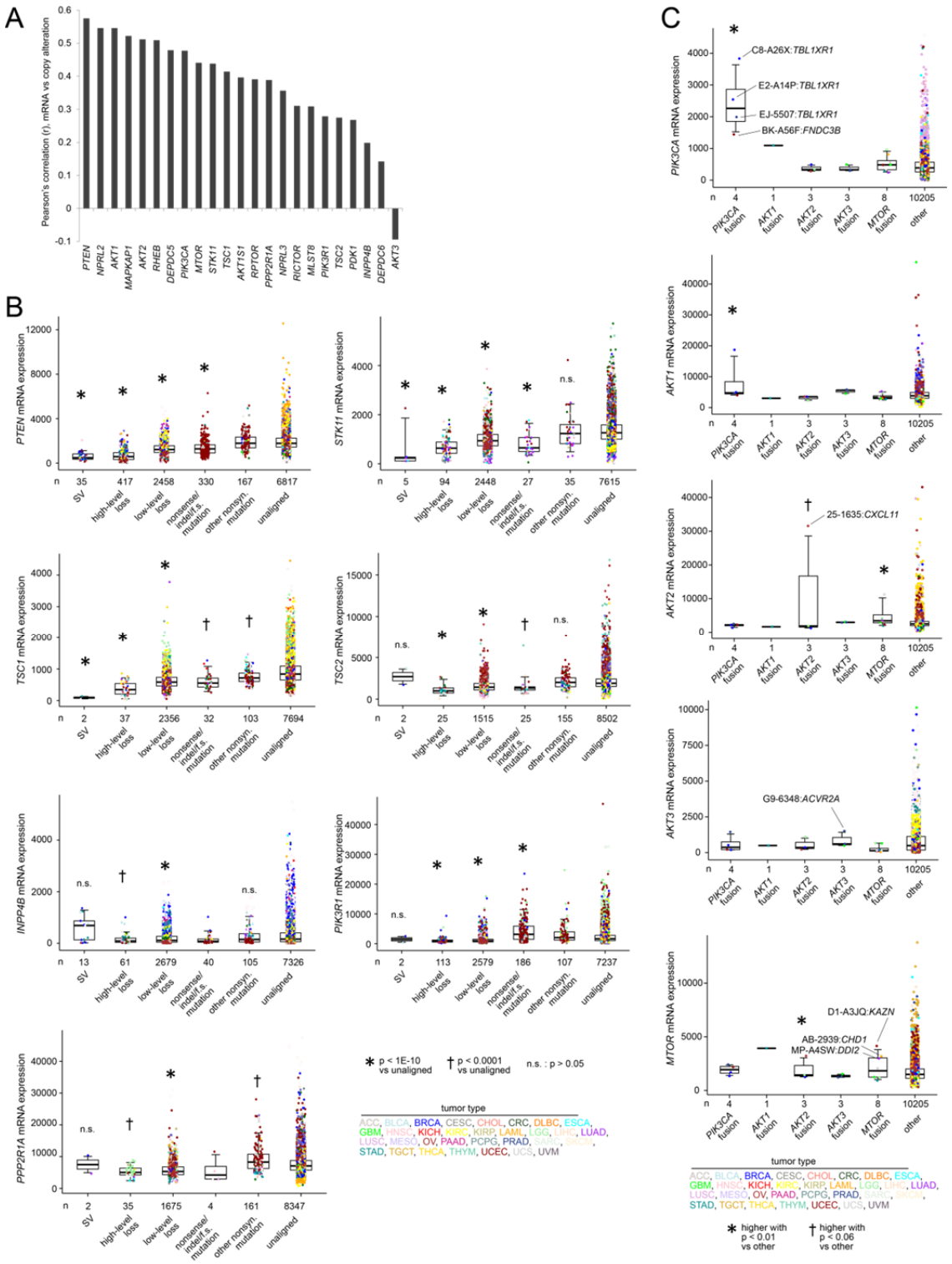

Figure S2, related to Figure 2. Correlations between DNA alteration and expression involving PI3K/AKT/mTOR genes. (A) For genes in the PI3K/AKT/mTOR pathway (from Figure 2A), Pearson's correlation between copy alteration (by Log (tumor/normal) ratio) and mRNA expression, involving the 9981 cases with both copy and expression data. All

correlations shown are statistically significant (p<1E-18). **(B)** For selected genes with Structural Variants (SVs) found within them in a fraction of cases (from Figure 2C), box plots of mRNA expression by alteration class (SV, copy alteration, somatic mutation), for the set of 10224 cancers cases with mRNA expression data available. Box plots represent 5%, 25%, 50%, 75%, and 95%. P values by t-test on log-transformed values; n.s., not statistically significant (p>0.05). **(C)** Given candidate gene fusions involving *PIK3CA*, *AKT1*, *AKT2*, *AKT3*, or *MTOR* (Stransky et al., 2014; Yoshihara et al., 2014), box plots of mRNA expression for these genes by fusion class. Box plots represent 5%, 25%, 50%, 75%, and 95%. P values by t-test on log-transformed values.

Table S3, related to Figure 2. By patient, data for key somatic mutation, copy alteration, and structural variant (SV) features examined in this study. Provided as an Excel file.

Table S4, related to Figure 2. For key genes, numbers of mutation events by cancer type. Provided as an Excel file.

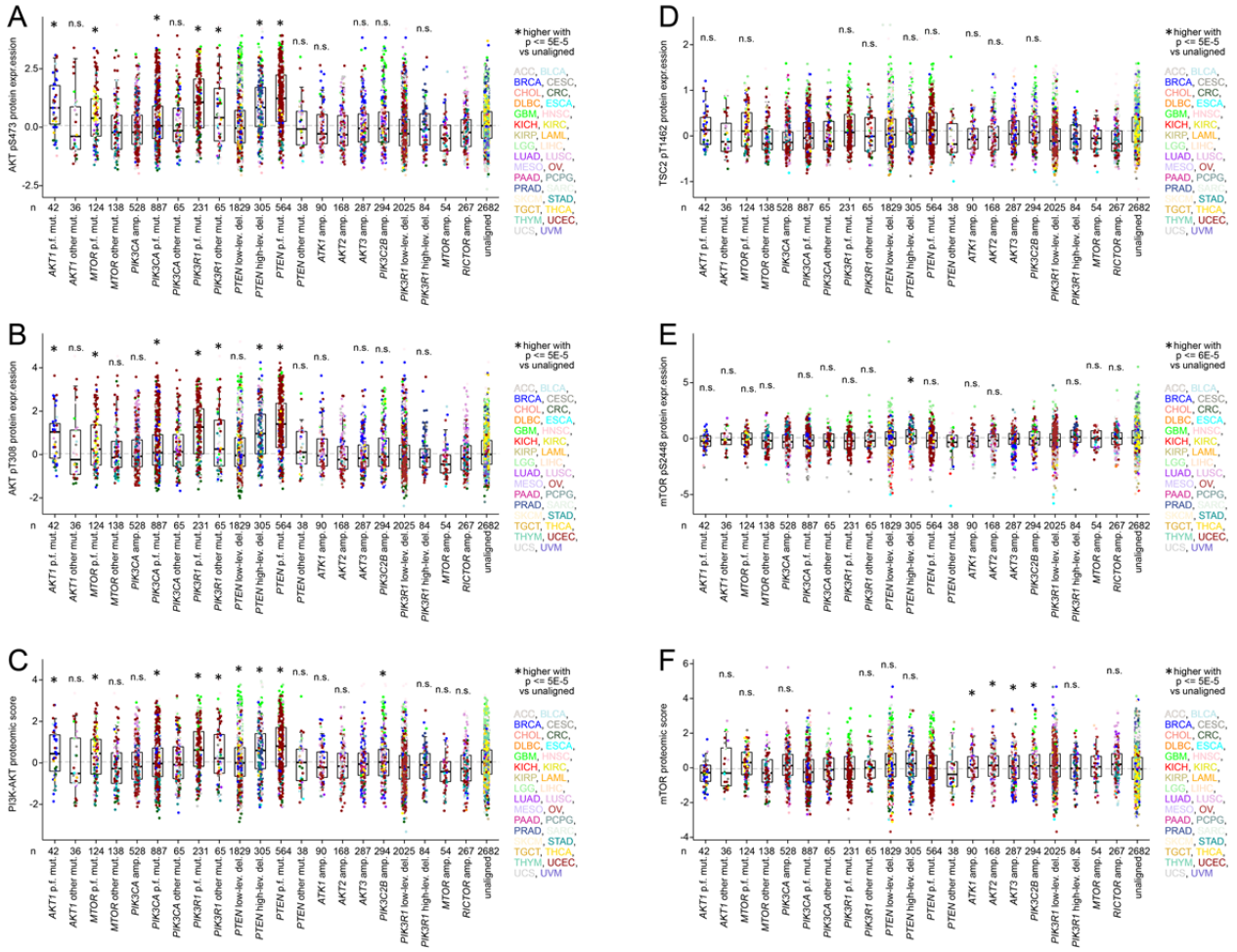

Figure S3, related to Figure 3. Association with PI3K/AKT/mTOR-related phospho-protein signaling of specific DNA alterations in genes having roles in AKT activation. **(A)** Box plot of AKT pS473 phospho-protein expression by mutation ("mut.") or copy alteration class, with the "unaligned" cases having none of the listed alteration types. "p.f." denotes "predicted functional" mutations (by hotspot or by Mutation Assessor analysis or by literature review or by nonsense/frameshift/indel involving *PTEN* or *PIK3R1*); "amp." denotes high-level gene amplification; "low-lev." and "high-lev.", low-level and high-level copy deletions, respectively. P values by t-test on log-transformed values. n.s., not significant (p>0.05). Box plots represent 5%, 25%, 50%, 75%, and 95%. Points in box plots are colored according to tumor type as defined by TCGA project as indicated. Most alteration classes shown here are also represented in Figures 7A and S5B, where aggregate levels of PI3K-AKT and mTOR signaling and a "HIGH P-AKT" alteration class are considered. **(B)** Similar to part A, but for AKT pT308 levels. **(C)** Similar to part A, but for PI3K-AKT aggregated proteomic score (from Figure 1A). **(D)** Similar to part A, but for TSC2 pT1462 levels. **(E)** Similar to part A, but for mTOR pS2448 levels. **(F)** Similar to part A, but for mTOR aggregated proteomic score (from Figure 1A).

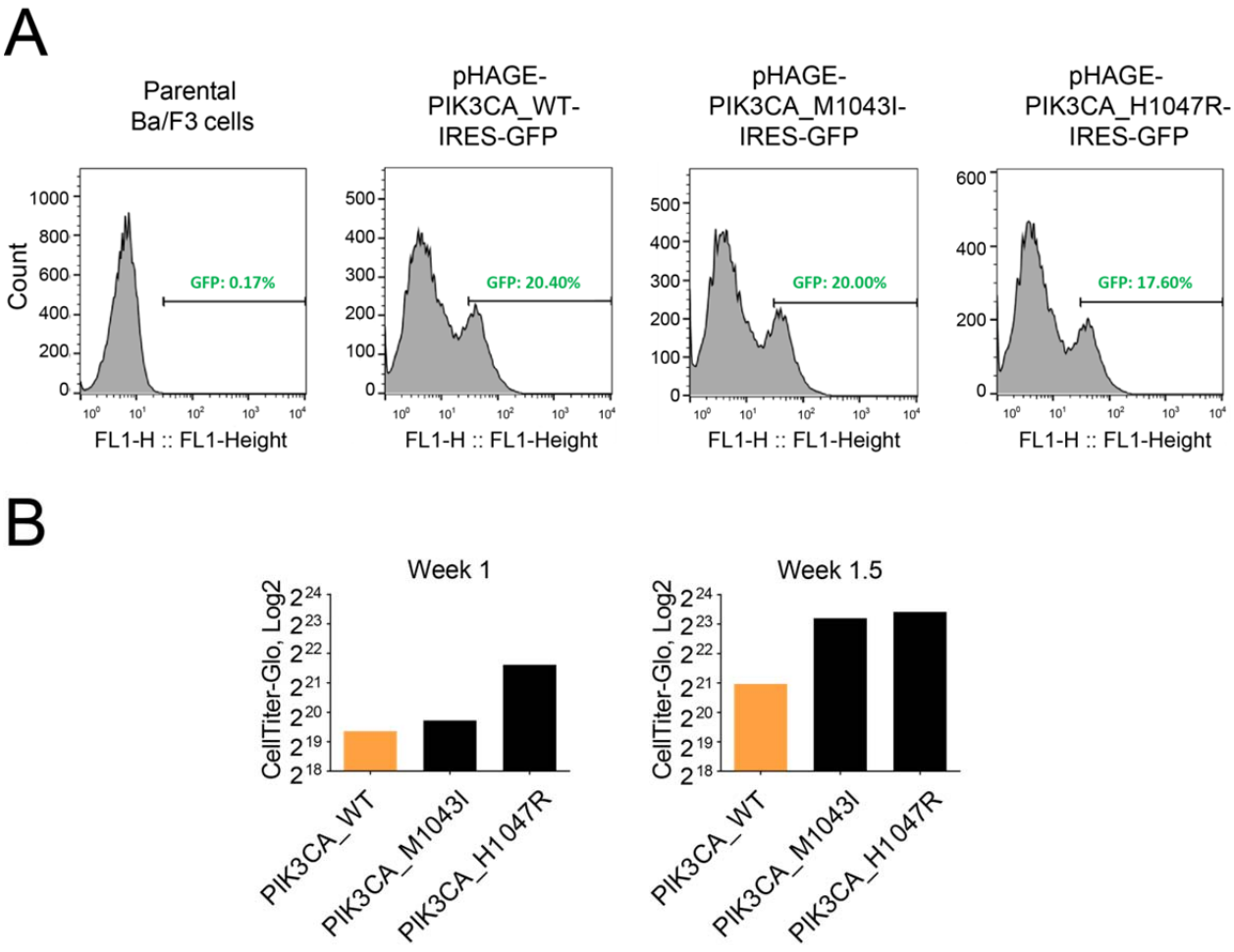

Figure S4, related to Figure 4. Quantitative measures underlying the functional assay calls made for specific variants. (A) *PIK3CA* WT, M1043I and H1047R were introduced into Ba/F3 cells using lentivirus approach. Transduced cells were incubated in assay medium for 3 days and subjected to FACS flow cytometry analysis. The transduction efficiency is represented by the percentage of GFP positive cells as showed in the graphs. The result showed that transductions of different plasmids have similar efficiency (ranged from 17.6% to 20.4%). No correlation between transduction efficiency and functional calls is observed. **(B)** Cell viability assay of transduced Ba/F3 cells 1 and 1.5 week(s) post-transduction was measured using CellTiter-Glo assay. Increased cell viability of H1047R and M1043I transduced cells were detected in week 1 and week 1.5, respectively, indicating that H1047R is a more active mutant than M1043I.

Table S5, related to Figure 4. Somatic mutation variants detected for PI3K/AKT/mTOR pathway members, annotated for frequency in TCGA cohort, expression of key protein features, hotspot residue according to Chang *et al*., Mutation Assessor algorithm, functional assay data (where available), and additional literature assessment. The CellTiter-Glo data of PIK3CA and PIK3R1 mutants are also provided here. Provided as an Excel file.

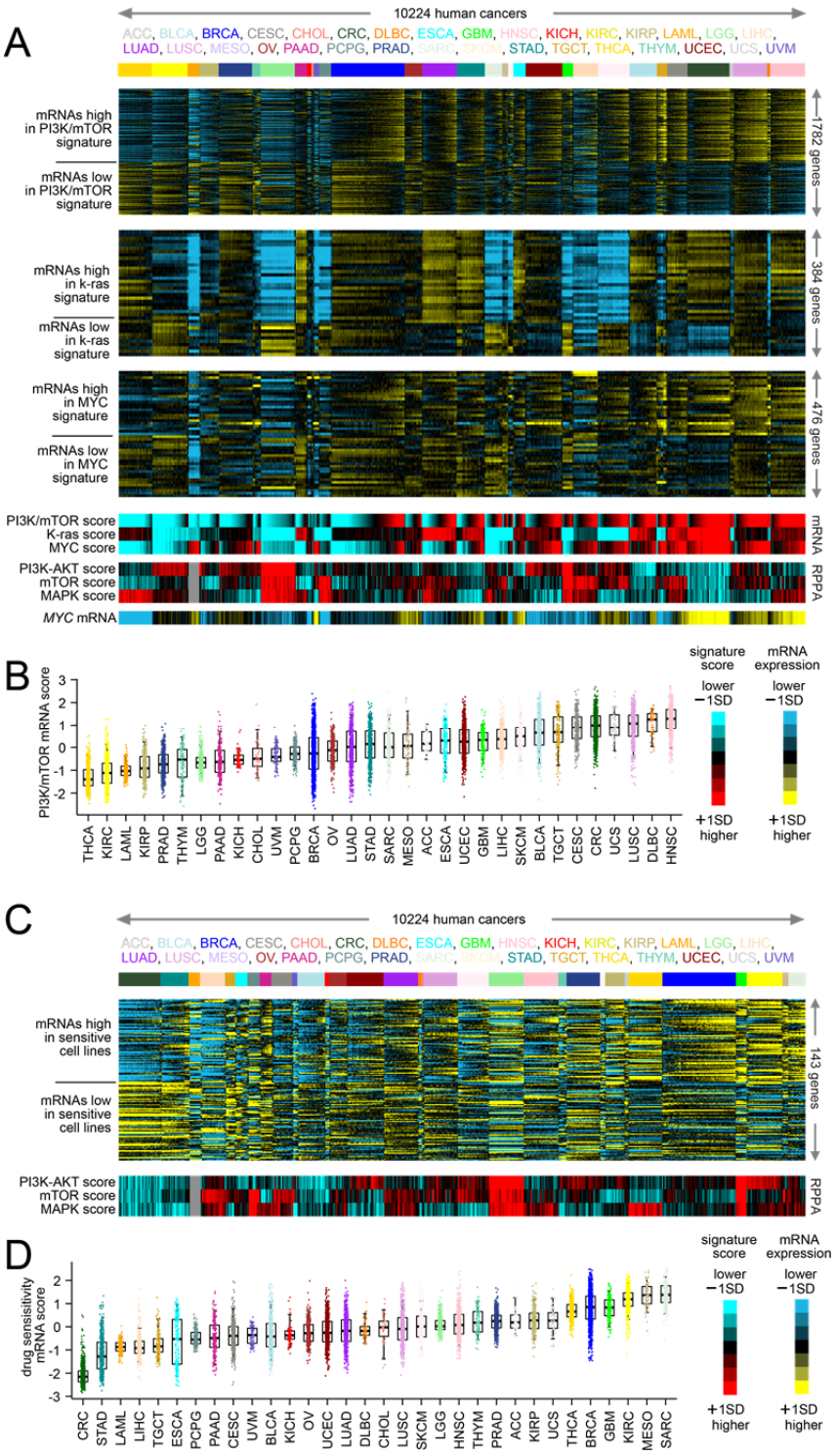

Figure S5, related to Figure 5. PI3K/AKT/mTOR-associated gene transcription signatures across TCGA human cancer profiles, by cancer type. (A) Heat map of genes in transcriptional signatures previously associated with PI3K/mTOR (Creighton et al., 2010), k-ras (Singh et al., 2009), or MYC (Coller et al., 2000), across 10224 cancers in TCGA for which RNA-seq data were available. Yellow, higher expression (relative to median across all cancers);

blue, lower expression; bright yellow/blue denotes change of 1 standard deviation (SD) from the median. Transcriptional signatures represented here were each summarized into pathway scores for each tumor profile (red, higher inferred activity; blue, lower activity). Cancer types (denoted by TCGA project name) are ordered by low to high average PI3K/mTOR transcriptional signature score. RPPA-based signature scores for PI3K/AKT, mTOR, and MAP kinase are also represented. **(B)** Box plots of PI3K/mTOR transcriptional signature scores, as inferred using RNA-seq data. **(C)** Heat map of genes in transcriptional signature of sensitivity to PI3K/AKT/mTOR inhibition in cancer cell lines (defined in main Figure 5D), across 10224 cancers in TCGA for which RNA-seq data were available. Yellow, higher expression (relative to median across all cancers); blue, lower expression; bright yellow/blue denotes change of 1 standard deviation (SD) from the median. Cancer types (denoted by TCGA project name) are ordered by low to high average transcriptional signature scoring for PI3K/AKT/mTOR inhibitor sensitivity. RPPA-based signature scores for PI3K/AKT, mTOR, and MAP kinase are also represented. **(D)** Box plots of transcriptional signature scores for PI3K/mTOR inhibitor sensitivity, as inferred using RNA-seq data. Box plots represent 5%, 25%, 50%, 75%, and 95%.

Table S6, related to Figure 5. Gene transcription signatures associated with PI3K/AKT/mTOR pathway. Provided as an Excel file.

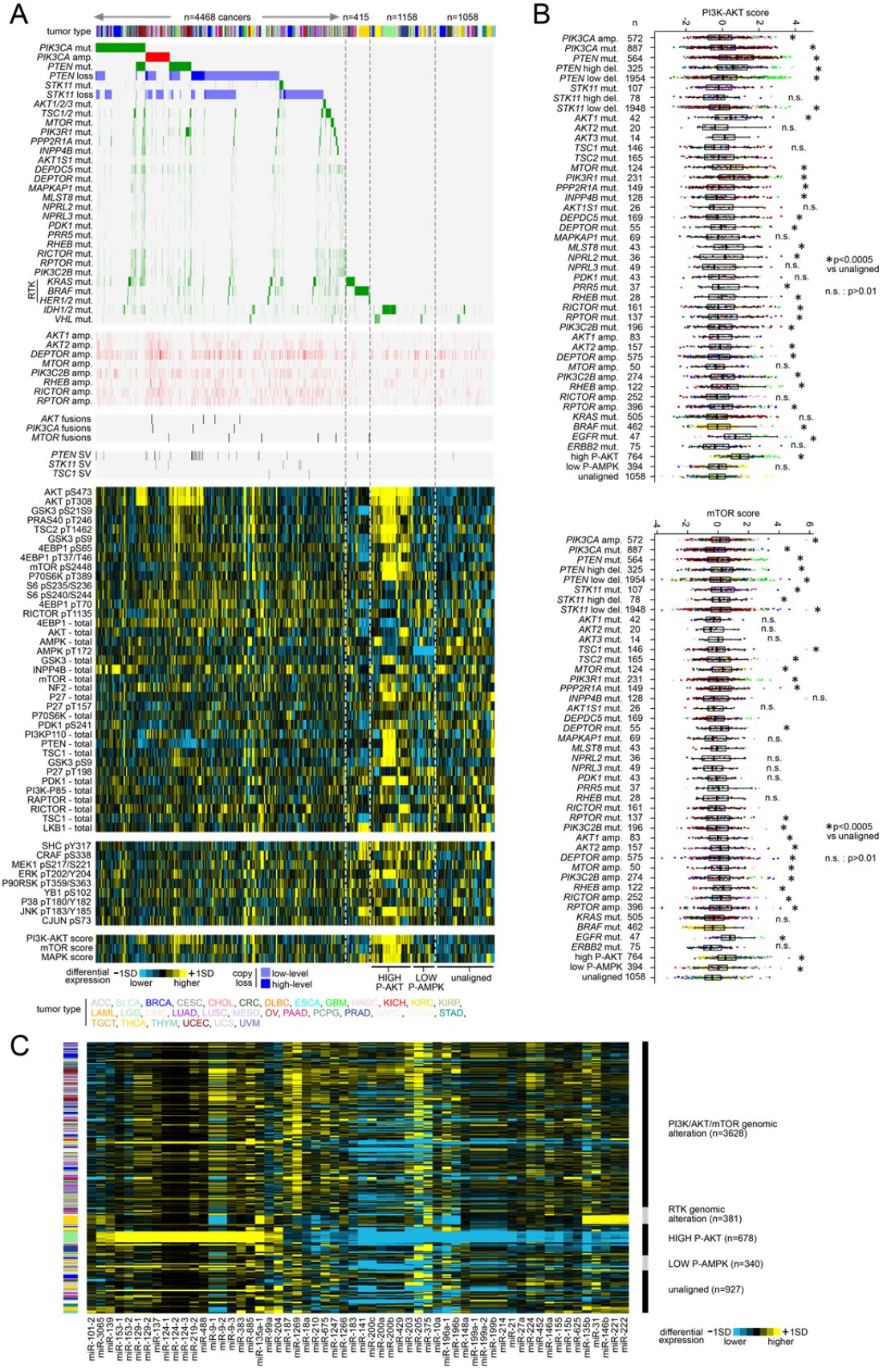
A
n=4468 cancers
n=415
n=1158
n=1058
tumor type
PIK3CA mut.
PIK3CA amp.
PTEN mut.
PTEN loss
STK11 mut.
STK11 loss
AKT1/2/3 mut.
TSC1/2 mut.
MTOR mut.
PIK3R1 mut.
PPP2R1A mut.
INPP4B mut.
AKT1S1 mut.
DEPDC5 mut.
DEPTOR mut.
MAPKAP1 mut.
MLST8 mut.
NPRL2 mut.
NPRL3 mut.
PDK1 mut.
PRR5 mut.
RHEB mut.
RICTOR mut.
RPTOR mut.
PIK3C2B mut.
RTK
KRAS mut.
BRAF mut.
HER1/2 mut.
IDH1/2 mut.
VHL mut.
AKT1 amp.
AKT2 amp.
DEPTOR amp.
MTOR amp.
PIK3C2B amp.
RHEB amp.
RICTOR amp.
RPTOR amp.
AKT fusions
PIK3CA fusions
MTOR fusions
PTEN SV
STK11 SV
TSC1 SV
AKT pS473
AKT pT308
GSK3 pS21S9
PRAS40 pT246
TSC2 pT1462
GSK3 pS9
4EBP1 pS65
4EBP1 pT37/T46
mTOR pS2448
P70S6K pT389
S6 pS235/S236
S6 pS240/S244
4EBP1 pT70
RICTOR pT1135
4EBP1 - total
AKT - total
AMPK - total
AMPK pT172
GSK3 - total
INPP4B - total
mTOR - total
NF2 - total
P27 - total
P27 pT157
P70S6K - total
PDK1 pS241
PI3KP110 - total
PTEN - total
TSC1 - total
GSK3 pS9
P27 pT198
PDK1 - total
PI3K-P85 - total
RAPTOR - total
RICTOR - total
TSC1 - total
LKB1 - total
SHC pY317
CRAF pS338
MEK1 pS217/S221
ERK pT202/Y204
P90RSK pT359/S363
YB1 pS102
P38 pT180/Y182
JNK pT183/Y185
CJUN pS73
PI3K-AKT score
mTOR score
MAPK score
differential expression
−1SD
+1SD
lower
higher
copy loss
low-level
high-level
HIGH P-AKT
LOW P-AMPK
unaligned
tumor type
ACC, BLCA, BRCA, CESC, CHOL, CRC, DLBC, ESCA, GBM, HNSC, KICH, KIRC, KIRP, LAML, LGG, LIHC, LUAD, LUSC, MESO, OV, PAAD, PCPG, PRAD, READ, SARC, STAD, TGCT, THCA, THYM, UCEC, UCS, UVM
B
PI3K-AKT score
n
PIK3CA amp. 572
PIK3CA mut. 887
PTEN mut. 564
PTEN high del. 325
PTEN low del. 1954
STK11 mut. 107
STK11 high del. 78
STK11 low del. 1948
AKT1 mut. 42
AKT2 mut. 20
AKT3 mut. 14
TSC1 mut. 146
TSC2 mut. 165
MTOR mut. 124
PIK3R1 mut. 231
PPP2R1A mut. 149
INPP4B mut. 128
AKT1S1 mut. 26
DEPDC5 mut. 169
DEPTOR mut. 55
MAPKAP1 mut. 69
MLST8 mut. 43
NPRL2 mut. 36
NPRL3 mut. 49
PDK1 mut. 43
PRR5 mut. 37
RHEB mut. 28
RICTOR mut. 161
RPTOR mut. 137
PIK3C2B mut. 196
AKT1 amp. 83
AKT2 amp. 157
DEPTOR amp. 575
MTOR amp. 50
PIK3C2B amp. 274
RHEB amp. 122
RICTOR amp. 252
RPTOR amp. 396
KRAS mut. 505
BRAF mut. 462
EGFR mut. 47
ERBB2 mut. 75
high P-AKT 764
low P-AMPK 394
unaligned 1058
n.s.
*p<0.0005 vs unaligned
n.s. : p>0.01
mTOR score
PIK3CA amp. 572
PIK3CA mut. 887
PTEN mut. 564
PTEN high del. 325
PTEN low del. 1954
STK11 mut. 107
STK11 high del. 78
STK11 low del. 1948
AKT1 mut. 42
AKT2 mut. 20
AKT3 mut. 14
TSC1 mut. 146
TSC2 mut. 165
MTOR mut. 124
PIK3R1 mut. 231
PPP2R1A mut. 149
INPP4B mut. 128
AKT1S1 mut. 26
DEPDC5 mut. 169
DEPTOR mut. 55
MAPKAP1 mut. 69
MLST8 mut. 43
NPRL2 mut. 36
NPRL3 mut. 49
PDK1 mut. 43
PRR5 mut. 37
RHEB mut. 28
RICTOR mut. 161
RPTOR mut. 137
PIK3C2B mut. 196
AKT1 amp. 83
AKT2 amp. 157
DEPTOR amp. 575
MTOR amp. 50
PIK3C2B amp. 274
RHEB amp. 122
RICTOR amp. 252
RPTOR amp. 396
KRAS mut. 505
BRAF mut. 462
EGFR mut. 47
ERBB2 mut. 75
high P-AKT 764
low P-AMPK 394
unaligned 1058
n.s.
*p<0.0005 vs unaligned
n.s. : p>0.01
C
PI3K/AKT/mTOR genomic alteration (n=3628)
RTK genomic alteration (n=381)
HIGH P-AKT (n=678)
LOW P-AMPK (n=340)
unaligned (n=927)
differential expression
−1SD
+1SD
lower
higher

Figure S6, related to Figure 7. Tumor classes as defined by PI3K/AKT/mTOR-related alterations, with expanded view involving additional related genomic features. (A) Genomic and proteomic features from Figure 7A, with additional features potentially relevant to PI3K/AKT/mTOR pathway, including high-level amplification events (*AKT1*, *AKT2*, *DEPTOR*, *MTOR*, *PIK3C2B*, *PIK3CA*, *RHEB*, *RICTOR*, *RPTOR*), gene fusions (involving *AKT*, *PIK3CA*, or *MTOR*, from (Stransky et al., 2014; Yoshihara et al., 2014)), SVs (involving *PTEN*, *STK11*, *TSC1*), and RPPA features related to PI3K/AKT/mTOR or MAP Kinase pathways. **(B)** Box plots of PI3K/AKT (top) and mTOR (bottom) pathway activity scores by alteration class. P values by t-test on log-transformed values. n.s., not significant ($p>0.01$). Box plots represent 5%, 25%, 50%, 75%, and 95%. **(C)** Top differentially expressed microRNAs (fold change >2 and $p<0.001$ by t-test on log-transformed data, comparing High P-AKT/Low P-AMPK tumors with PI3K/RTK genomic altered tumors and with unaligned tumors) associated with different groups of cases as defined above.

REFERENCES

Coller, H. A., Grandori, C., Tamayo, P., Colbert, T., Lander, E. S., Eisenman, R. N., and Golub, T. R. (2000). Expression analysis with oligonucleotide microarrays reveals that MYC regulates genes involved in growth, cell cycle, signaling, and adhesion. Proc Natl Acad Sci USA *97*, 3260-3265.

Creighton, C., Fu, X., Hennessy, B., Casa, A., Zhang, Y., Gonzalez-Angulo, A., Lluch, A., Gray, J., Brown, P., Hilsenbeck, S.*, et al.* (2010). Proteomic and transcriptomic profiling reveals a link between the PI3K pathway and lower estrogen-receptor (ER) levels and activity in ER+ breast cancer. Breast Cancer Res *12*, R40.

Singh, A., Greninger, P., Rhodes, D., Koopman, L., Violette, S., Bardeesy, N., and Settleman, J. (2009). A gene expression signature associated with "K-Ras addiction" reveals regulators of EMT and tumor cell survival. Cancer Cell *15*, 489-500.

Stransky, N., Cerami, E., Schalm, S., Kim, J., and Lengauer, C. (2014). The landscape of kinase fusions in cancer. Nat Commun *5*, 4846.

Yoshihara, K., Wang, Q., Torres-Garcia, W., Zheng, S., Vegesna, R., Kim, H., and Verhaak, R. (2014). The landscape and therapeutic relevance of cancer-associated transcript fusions. Oncogene *E-pub 2014 Dec 15*.